Available online at www.sciencedirect.com

ScienceDirect

Physics Procedia 64 (2015) 83 – 90

Physics Procedia

Scientific Workshop on Nuclear Fission Dynamics and the Emission of Prompt Neutrons and Gamma Rays, THEORY-3

Prompt fission γ-ray spectra characteristics - a first summary

S. Oberstedt[a,*], R. Billnert[a,b], A. Gatera[a], W. Geerts[a], P. Halipré[c], F.-J. Hambsch[a], M. Lebois[c], A. Oberstedt[b,d], P. Marini[e], M. Vidali[a], J.N. Wilson[c]

[a]*European Commission, DG Joint Research Centre (IRMM), 2440 Geel, Belgium*
[b]*Fundamental Fysik, Chalmers Tekniska Högskola, 41296 Göteborg, Sweden*
[c]*Institut de Physique Nucléaire Orsay, 91406 Orsay, France*
[d]*OSSOLUTIONS Consulting, 70353 Örebro, Sweden*
[e]*Centre d'Etudes Nucléaires de Bordeaux Gradignan, 33175 Gradignan Cedex, France*

Abstract

In this work we give an overview of our investigations of prompt γ-ray emission in nuclear fission. This work was conducted during the last five years in response to a high priority nuclear data request formulated by the OECD/NEA. The aim was to reveal data deficiencies responsible for a severe under-prediction of the prompt γ heating in nuclear reactor cores. We obtained new prompt fission γ-ray spectral (PFGS) data for ^{252}Cf(SF) as well as for thermal-neutron induced fission on ^{235}U(n$_{th}$,f) and ^{241}Pu(n$_{th}$,f). In addition, first PFGS measurements with a fast-neutron beam were accomplished, too. The impact of the new data and future data needs are discussed.

Peer-review under responsibility of the European Commission, Joint Research Centre – Institute for Reference Materials and Measurements

Keywords: Prompt fission γ-rays; total γ-ray energy; prompt γ-ray multiplicity; Generation IV; nuclear energy; lanthanum bromide; cerium bromide; scintillation detector; ^{252}Cf(SF); ^{235}U(n$_{th}$,f); ^{241}Pu(n$_{th}$,f);

1. Introduction

In nuclear fission around 99.8% is binary fission, where a total energy of around 200 MeV is released. About 80% appears as kinetic energy of the two fission fragments. The fragments may be highly excited, the excitation energy of each fragment ranging between 0 and 40 MeV. About 40% of the excitation energy is released shortly after scission through the emission of neutrons and γ-rays, in average about 5 and 7 MeV, respectively. All energy release before the onset of β^--decay is defined as *prompt* heat. The regime of prompt emission may, therefore, comprise several hundreds of *n*s and even extend into the 100 μs range.

* Corresponding author. Tel.: +32-14-571-361 ; fax: +32-14-571 862.
E-mail address: stephan.oberstedt@ec.europa.eu

Peer-review under responsibility of the European Commission, Joint Research Centre – Institute for Reference Materials and Measurements
doi:10.1016/j.phpro.2015.04.011

In order to understand the share of excitation energy between the two fission fragments, prompt neutrons and γ-rays are excellent probes to investigate the re-organization of nuclear matter around scission and the subsequent de-excitation process. Whilst prompt-neutron emission is being studied along the last three decades (Boikov et al., 1991; Lemaire et al., 2005; Kornilov et al., 2010; Tudora et al., 2013), prompt γ-ray measurements date back to the early 1970s (Verbinski et al., 1973; Pleasonton et al., 1972; Peelle and Maienschein, 1971) and have been disregarded until in the very recent years. However, the latter probe may, however, help revealing in how far prompt neutron and γ emission is a competing process. Depending on the excitation energy and the angular momentum of a fragment with mass A and its decay product, with mass A-1, neutron emission is favored or suppressed. Those quantities are not directly experimentally assessable but may be deduced by comparing model calculations with neutron and γ-ray spectral data.

2. Prompt fission γ-ray emission - the "why"

Regardless the fundamental aspects of prompt fission neutron and γ-ray emission, the driving force for a renaissance of prompt fission γ-ray measurements was the community of nuclear applications. Since four out of six impending Generation-IV reactors will be operated with a fast-neutron spectrum, modeling of innovative reactor cores is required to handle the excessive heat deposit during operation. Model calculations consistently under-predicted the prompt heat deposition by up to 28% (Rimpault et al., 2006, 2012; Rimpault, 2006b). Since the under-prediction was attributed to deficiencies in the prompt fission γ-ray spectral (PFGS) data from thermal-neutron induced fission on ^{235}U as well as on ^{239}Pu, the OECD/NEA published a high priority nuclear data request in 2006 (NEA, 2006). New data on the average prompt γ-ray energy per fission should be measured within an uncertainty of 7.5% for thermal- and fast-neutron induced fission.

In the following we summarize the subsequent activities and present, in the following, recent achievements in measuring PFGS data, average multiplicity (ν_γ), mean photon energy (ϵ_γ) and average total γ-ray energy ($\overline{E}_{\gamma,tot}$) per fission.

3. Experiment technique - the "how"

For the investigation of prompt fission γ-rays an efficient separation from prompt fission neutrons must be achieved. Those neutrons may interact with the fission chamber and surrounding materials as well as with the γ-detector through inelastic scattering, causing the detection of γ-rays to be confounded with prompt fission γ-rays. This separation is usually achieved by means of time-of-flight. This method requires an excellent timing resolution allowing to use a not too large distance between fission source and γ-detector. A crucial point is the, in general, not negligible amount of material around a fission source itself, e.g. material from a diamond detector mounted close to the sample or from a (twin) Frisch-grid ionization chamber (TFGIC), which requires sufficiently high energy resolution as well.

Of the historically employed detectors that based e.g. on thallium-doped sodium-iodine crystals possesses of both characteristics to a certain extent. With the newly emerged cerium-doped lanthanum halide, e.g.$LaBr_3$:Ce and $LaCl_3$:Ce, and cerium-halide, e.g. $CeBr_3$, crystals the situation improved considerably. Before we started with PFGS measurements we investigated the characteristics of those detectors with respect to energy and timing resolution (Billnert et al., 2011, 2012; Oberstedt et al., 2013; Billnert et al., 2013), which we found superior by a factor of 2 and 5, respectively. Also the detection efficiency is higher by a factor of about 2. The reproducibility of spectral data measurements lies within a few percent as demonstrated with the spontaneous fission of ^{252}Cf, where PFGS data were measured with different lanthanide-halide detectors of different sizes (Oberstedt et al., 2014b).

In the left part of Fig. 1 a typical setup for PFGS measurements is shown as it was used at the KFKI research reactor at Budapest (KFKI, 2014). As a fission trigger we used artificial diamond detectors, which provide an intrinsic timing resolution better than 110 ps (σ) (Oberstedt et al., 2013c) or a TFGIC, when fission-fragment characteristics were to be measured in correlation with prompt fission γ-rays. A coincidence timing resolution between γ-detector and fission trigger better than 2 ns (FWHM) may routinely be achieved when integrating over all γ-ray energies (Oberstedt et al.,

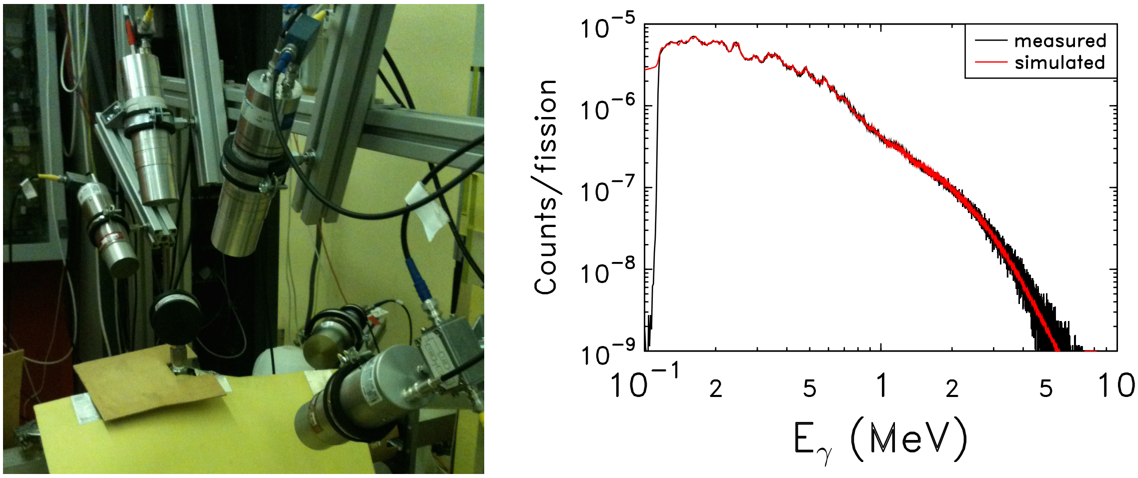

Fig. 1. (Color online) Left: Typical set-up for measuring prompt fission γ-rays at the cold-neutron beam at the KFKI research reactor in Budapest. The fissile actinide sample is mounted in a Frisch-grid ionization chamber covered here by (yellow) ^{6}Li-loaded sheets to minimize neutron scattering into the detectors; Right: Measured prompt fission γ-ray spectrum (black) from ^{252}Cf(SF) and the spectrum simulated with the PENELOPE Monte-Carlo code (PENELOPE, 2011).

2014).

Data are collected with an acquisition system based on wave-form digitization. We store the entire signal trace released from each γ-ray or fission detector using M3i digitizer cards (400 Ms/s, 12bit) from Spectrum (Spectrum, 2011), ^{252}Cf(SF) and ^{235}U(n$_{th}$,f), while during the measurement on ^{241}Pu digitizer boards from SPDevices with 400 Ms/s and 14 bit resolution (SPDevices, 2012) were used. The recorded traces were then treated off-line using a ROOT-based analysis program (ROOT, 2014) developed at the Joint Research Centre IRMM.

The measured γ-ray spectrum was corrected for the detector response, which was simulated for each detector type and size by means of the PENELOPE Monte-Carlo code (PENELOPE, 2011). Up to 200 γ-ray energies were simulated between 50 keV and 12 MeV. The distance between each simulated energy corresponded to the energy resolution of the corresponding detector. Each simulated γ-ray energy was then fitted to the measured spectrum until minimization of χ^2 was achieved (see Fig. 1, right part). The sum of all fitted intensities for each γ-line represents the PFG emission spectrum, from which we calculate the characteristic parameters average multiplicity (ν_γ), mean photon energy (ϵ_γ) and average total γ-ray energy ($\overline{E}_{\gamma,tot}$) per fission, viz (Oberstedt et al., 2014).

4. Prompt fission γ-ray data - the "achievements"

During the last three years new PFGS for the spontaneous fission of ^{252}Cf (Billnert et al., 2013) and thermal-neutron induced fission of ^{235}U (Oberstedt et al., 2013b) and ^{241}Pu (Oberstedt et al., 2014) were obtained. In Fig. 2 the low-energy part of the emission spectrum obtained from the spontaneous fission of ^{252}Cf is shown (red symbols and full line) and compared to the historical data from (Verbinski et al., 1973) (blue dashed line). We observe a similar structure in the spectrum, which is more complex thanks to the better energy resolution of lanthanide-halide detectors. The additional structure below about 0.2 MeV appears due to a lower pulse-height threshold achieved in our measurements. Figure 2 also includes the latest evaluated spectrum in (ENDF/B-VII.1, 2011) (dotted line) and a recent model calculation performed with the Monte-Carlo code FIFRELIN (Regnier et al., 2012; Regnier, 2013) shown as full black line. The model calculation is able to reproduce well the observed structure and rules out the structureless and, hence, unphysical evaluation. The PFGS characteristics for our investigated fissioning systems are summarized in Tab. 1. We compare the results with corresponding data from the (ENDF/B-VII.1, 2011) library and quantify the observed differences in the third line for each investigated system. In all systems studied up to this point we observe

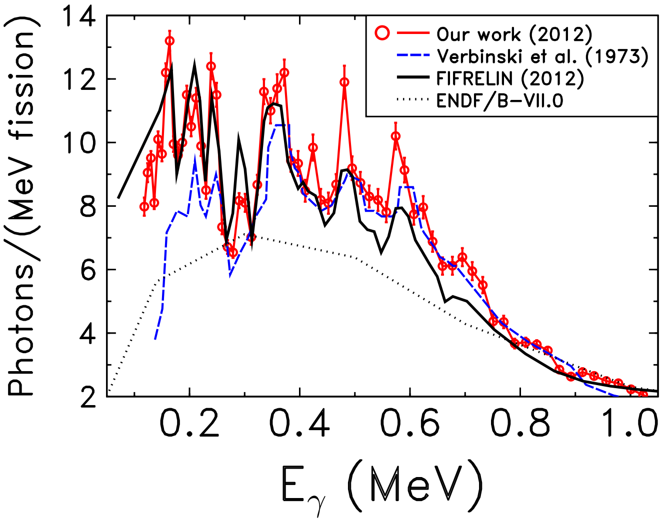

Fig. 2. (Color online) Prompt fission γ-ray spectrum from the spontaneous fission from ^{252}Cf (Billnert et al., 2013) compared to the historical data of Verbinski et al. (Verbinski et al., 1973) and recent FIFRELIN model calculations (Regnier, 2013). The dotted line represents the evaluated data (ENDF/B-VII.1, 2011).

Table 1. Summary of our results compared to present ENDF/B-VII.1 data. The relative difference is how the evaluated data needs to change to correspond to our measurement.

Reaction	Dataset	Multiplicity /fission	γ-energy released MeV/Fission
^{252}Cf(SF)	Our measurement	8.29(6)	6.63(8)
	ENDF/B-VII.1	7.85	6.13
	Relative difference	+5.6%	+8.2%
^{235}U(n$_{th}$,f)	Our measurement	8.19(11)	6.92(9)
	ENDF/B-VII.1	6.86	6.58
	Relative difference	+19.3%	+5.2%
^{241}Pu(n$_{th}$,f)	Our measurement	8.21(9)	6.41(6)
	ENDF/B-VII.1	8.18	6.19
	Relative difference	+1.3%	+3.6%

an excess in the released average total γ-ray energy per fission of a few percent. If we make a reasonable assumption that the excess in the reaction ^{239}Pu(n$_{th}$, f) is not dramatically higher than the one in the studied reaction on ^{241}Pu, the observed excess cannot explain the under-predicted prompt γ heat in the cores of nuclear reactors as suggested in (Rimpault et al., 2006, 2012; Rimpault, 2006b). In consequence, other reactions should be considered as well, as e.g. fast-neutron induced fission on ^{235}U and ^{239}Pu, but certainly on ^{238}U, which represents the main component in the nuclear fuel.

For the investigation of the above suggestion we are being developing a forward-directed fast-neutron beam based on the reaction H(^{7}Li, n)^{7}Be enabling the placement of a large number of γ-ray detectors in close geometry with the fissioning sample outside the fast-neutron beam (Lebois et al., 2014). This novel neutron source, called LICORNE (Lithium Inverse Cinematiques ORsay NEutron source), is installed at the tandem accelerator of the Institut de Physique Nucléaire in Orsay, France. Spectra from a first measurement on ^{235,238}U(n, f) at an average neutron energy $\overline{E}_n$ = 1.5 MeV are shown in Fig. 3 for illustration. PFGS data were taken with two different sets of detectors, one consisting of two clusters of 7 BaF_2 detector with a size 10 cm × 15 cm (diameter × length) each (red lines) and another made from three individual $LaBr_3$:Ce detectors of size 5 cm × 5 cm (diameter × length) and shown as green dashed lines. In the left part of Fig. 3 the spectrum measured at thermal neutron energy (blue line) is shown for

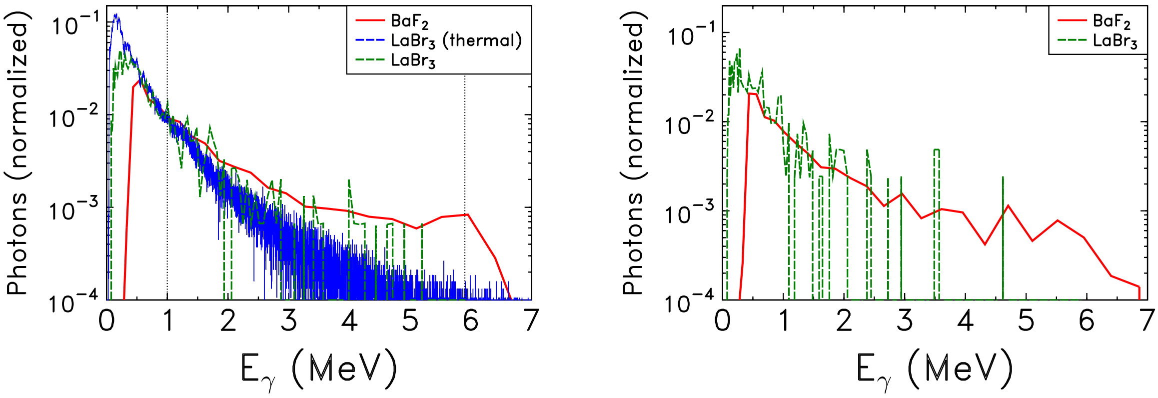

Fig. 3. (Color online) Left: Measured prompt γ-ray spectra for the neutron induced fission on ^{235}U; the red full and green dashed line depicts the spectrum obtained from fats-neutron induced fission at LICORNE taken with the BaF_2 detector clusters and the $LaBr_3$:Ce as explained in the text. The blue dashed curve gives the corresponding spectrum obtained from thermal-neutron induced fission. (Oberstedt et al., 2013b). Right: Measured prompt γ-ray spectrum for fast-neutron induced fission on ^{238}U again for the two different detector systems.

comparison. The spectral shape looks very good albeit the much smaller number of events in the spectrum and the higher pulse-height threshold. The right part of Fig. 3 depicts the corresponding PFGS for the reaction ^{238}U. Details on the LICORNE facility and the PFGS measurements are subject to another contribution in this issue of Physics Procedia (Wilson et al., 2014b).

The low-energy structure observed in the PFGS from ^{252}Cf(sf) is also visible in the spectra from thermal-neutron induced fission on ^{235}U and ^{241}Pu with the individual peaks showing different intensities (Oberstedt et al., 2013b, 2014). This may be due to the different shape of the corresponding mass distributions. To study this intriguing feature of the PFGS in more detail we started measuring the spontaneous fission of ^{252}Cf with focus on correlations of PFGS with fission-fragment properties, in particular on the link between the (low-energy) structure and particular mass splits, and on whether the PFGS characteristics change significantly as a function of mass.

In a first step we measured PFGS as a function of the heavy fragment mass, in Fig. 4 shown for mass cuts of 2 mass units. Apart form the strongly changing structure at γ-ray energies below 1 MeV, we may observe a distinct shape change at mass splits with a heavy mass around or smaller than A = 132. A harder γ-ray spectrum was already observed in the 1990s (Hotzel et al., 1996) in an experiment with a 4π NaI-detector array and attributed to non-statistical γ-emission with $E_\gamma > 3.5$ MeV from spherical fission fragments. Our data shows that the shape change starts already around 2.5 MeV. Of course, more data is necessary for a quantitative explanation in terms of fission-fragment mass and total kinetic energy.

In a second step we started to look at isomeric γ-rays in fission fragments. In Figure 5 emission spectra for time cuts corresponding to 3 - 6 ns (red) and 7 - 10 ns (green) relative to the instant of fission are shown together with the prompt distribution for comparison (black line). Prompt and isomer spectra are corrected for the inelastic scattering of fission neutrons populating the first excited state in ^{56}Fe (E_γ = 0.847 MeV) present in the construction material of the fission chamber. Contributions from (n, n') in bromine isotopes present in the $LaBr_3$:Ce detectors at $E_\gamma \approx 0.28$ MeV can only be caused by fission neutrons with an energy of at least 8 MeV according to their time of flight. Their fraction is extremely small and does not affect the present spectra in a significant way.

In Fig. 5 some transitions are indicated, which are visible in the first isomer spectrum but not in the second. Therefore, one may put a stringent condition on the half-life of the decaying level. Together with the γ-ray energy fragment identification seems possible, at least in a few cases. This work is still ongoing and with a further increased number of events later time cuts are possible to be investigated allowing spectroscopy of very neutron-rich isotopes very close to scission and, more applied, determining the contribution of isomeric γ-decay to the prompt γ heating.

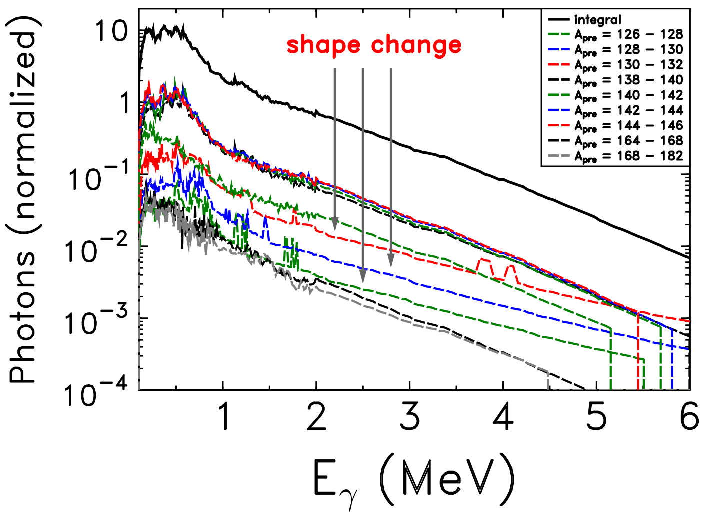

Fig. 4. (Color online) Prompt fission γ-ray spectra as a function of the heavy pre-neutron fission-fragment mass, A_{pre}, shown in logarithmic scale. Each mass cut contains also the contribution from the complementary light fragment, A_{comp}. Indicated is the significant spectral shape change around E_γ = 2.5 MeV for masses between A_{pre} = 126 and A_{pre} = 132 (including A_{comp} = 126 and A_{comp} = 120).

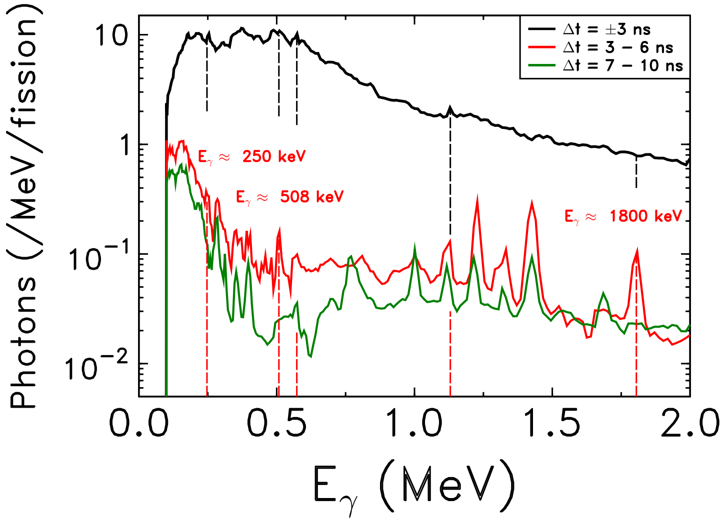

Fig. 5. (Color online) Fission γ-ray spectra for time cuts corresponding to 3 - 6 ns (red) and 7 - 10 ns (green) relative to the instant of fission together with the prompt distribution shown for comparison (black line). The vertical dotted lines indicate presumable isomeric transitions in fission fragments with half-lives well below 3 ns (see text for details).

5. Further data needs - the "future"

From the comparison of our new and precise prompt fission γ-ray data with the tabulated values in (ENDF/B-VII.1, 2011), cf. Tab. 1, we have to suspect that deficient data from other reactions contribute to the under-prediction of the prompt γ-heating in the core of a nuclear reactor. Although no new data from the reaction ^{239}Pu(n_{th}, f) were measured yet, we have no reason to assume significant deficiencies in the historical data from (Verbinski et al., 1973; Pleasonton et al., 1972). However, new measurements are scheduled for 2015.

A measurable contribution may be expected to come from the fast-neutron induced fission. Here not only the fissile isotopes have to be investigated in the future but also the non-fissile isotope ^{238}U, representing the major constituent of the nuclear fuel. These measurements have been started already at the novel directional neutron source LICORNE for neutron energies up to 4 MeV and will be pursued in 2015.

In addition, more isotopes should be investigated to reveal systematic trends as a function of incident neutron energy for the PFGS characteristics, average multiplicity (ν_γ), mean photon energy (ϵ_γ) and average total γ-ray energy ($\overline{E}_{\gamma,tot}$) per fission, viz. In (Oberstedt et al., 2014c) this work has been started based on the approach of (Valentine, 2001). PFGS measurements on spontaneously fissioning isotopes ^{240,242}Pu and ^{246,248}Cm are under way or in preparation at the JRC-IRMM.

The systematic investigation should be extended to photon-induced fission as well, which allows assessing different excitation regimes not (directly) accessible in neutron-induced fission. Moreover, fission induced from high-energy γ-rays from neutron capture in isotopes present in the construction materials close to the nuclear fuel is not even considered in present reactor calculations. It is tempting to estimate the possible contribution from this process to the total prompt heat production in the reactor.

Acknowledgements

Two of the authors (R. B. and A. G.) are indebted to the European Commission for providing a PhD fellowship at EC-JRC IRMM, during which part of this work was carried out. This work was also supported by the European Commission in the frame works of the FP7-ERINDA programme (agreement number 269499), which is hereby gratefully acknowledged. The authors are very grateful to the colleagues at the KFKI Budapest for their invaluable support during several measurement campaigns.

References

Billnert, R., Oberstedt, S., Andreotti, E., Hult, F.C., Marissens, G. , Oberstedt, A., 2011, Nucl. Instr. and Meth. A 647, 94.

Billnert, R., Andreotti, E. , Hambsch, F.-J., Hult, M., Karlsson, J., Marissens, G., Oberstedt, A., Oberstedt, S., 2012, Phys. Procedia 3, 29.

Billnert, R., Hambsch, F.-J., Oberstedt, A. and Oberstedt, S., 2013, Phys. Rev C87, 024601.

Boikov, G.S., Dmitriev, V.D., Kudyaev, G.A., Ostapenko, Yu.B., Svirin, M.I., and Smirenkin, G.N., 1991, Sov. J. Nucl. Phys. 53, 392.

Chyzh, A., Wu, C. Y., Kwan, E., Henderson, R. A., Gostic, J. M., Bredeweg, T. A., Haight, R. C., Hayes-Sterbenz, A. C., Jandel, M., ODonnell, J. M., and Ullmann, J. L., 2012, Phys. Rev. C 85, 021601.

ENDF/B-VII Evaluated Nuclear Data File ZA = 98251, MF = 15, MT = 18 (2011), http://www.nndc.bnl.gov/exfor/endf00.jsp.

Hotzel, A., Thirolf, P., Ender, Ch., Schwalm, D., Mutterer, M., Singer, P., Klemens, M., Theobald, J.P., Hesse., M., Gönnenwein, F., van den Ploeg, H., 1996, Z. Physik A - Hadrons and Nuclei 356, 299.

KFKI Research Reactor, Budapest (HU), http://www.bnc.hu

Kornilov, N., Hambsch, F.-J., Fabry, I., Oberstedt, S., Belgya, T., Kis, Z., Szentmiklosi, L., Simakov, S., 2010, Nucl. Sci. Engin. 165, 117.

Lebois, M., Wilson, J.N., Halipré, P., Leniau, B., Matea, I., Oberstedt, A., Oberstedt, S., 2014, Nucl. Inst. Meth. A 735, 145.

Lemaire, S., Talou, P., Kawano, T., Chadwick, M.B., and Madland, D.G., 2005, Phys. Rev. C 72, 024601.

Lutter, G., Hult, M., Billnert, R., Oberstedt, A., Oberstedt, S., Andreotti, E., Marissens, G., Rosengard, U., Tzika, F., 2013, Nucl. Instr. and Meth. A 703, 158.

Nuclear Data High Priority Request List of the NEA (Req. ID: H.3, H.4), http://www.nea.fr/html/dbdata/hprl/hprlview.pl?ID=421 and http://www.nea.fr/html/dbdata/hprl/hprlview.pl?ID= 422.

Oberstedt, A., Billnert, R., Oberstedt, S., 2013, Nucl. Instr. And Meth. A 708, 7.

Oberstedt, A., Belgya, T., Billnert, R., Borcea, R., Bryś, T., Geerts, W., Göök, A., Hambsch, F.-J., Kis, Z., Martinez, T., Oberstedt, S., Szentmiklosi, L., Takacs, K. and Vidali, M., 2013, Phys. Rev. C87, 051602(R).

Oberstedt, A., Billnert, R., Hambsch, F.-J., Oberstedt, S., submitted for publication.

Oberstedt, A., Billnert, R., Oberstedt, S., submitted for publication.

Oberstedt, S., Borcea, R., Bryś, T., Gamboni, Th., Geerts, W., Hambsch, F.-J., Oberstedt, A., Vidali, M., 2013, Nucl. Inst. Meth. A 714, 31.

Oberstedt, S., Billnert, R., Belgya, T., Bryś, T., Geerts, W., Guerrero, C., Hambsch, F.-J., Kis, Z., Moens, A., Oberstedt, A., Sibbens, G., Szentmiklosi, L., Vanleeuw, D. and Vidali, M., High precision prompt spectral γ-ray data from the reaction ^{241}Pu(n_{th}, f), 2014, Phys. Rev. C90, 024618.

Peelle, R.W. and Maienschein, F.C., 1971, Phys. Rev C3, 373.

PENELOPE 2011, http://www.oecd-nea.org/tools/abstract/detail/nea-1525.
Pleasonton, F., Ferguson, R.L. and Schmitt, H.W., 1972, Phys. Rev. C6, 1023.
Regnier, D., Litaize, O. and Serot, O., 2012, Physics Procedia 31, 59.
Regnier, D., 2013, private communication.
Rimpault, G., Courcelle, A. and Blanchet, D., 2006, Comment to the HPRL: ID H.3 and H.4.
Rimpault, G., Bernard, D., Blanchet, D., Vaglio-Gaudard, C., Ravaux, S., Santamaria, A., 2012, Phys. Procedia 31, 3.
Rimpault, G., 2006, Proc. Workshop on Nuclear Data Needs for Generation IV, April 2005 (Editor: P. Rullhusen) Antwerp, Belgium, World Scientic, ISBN 981-256-830-1, 46.
ROOT Data Analysis Framework, http://root.cern.ch (2014).
SP Devices, http://spdevices.com/.
Spectrum GmbH, http://spectrum-instrumentation.com/en.
Tudora, A., Hambsch, F.-J., and Oberstedt, S., 2013, Nucl. Phys. A 917, 43.
Valentine, T.E., 2001, Ann. Nucl. Energy 28, 191.
Verbinski, V.V., Weber, H. and Sund, R.E., 1973, Phys. Rev C7, 1173.
Wilson, J.N. et al., 2015, Physics Procedia, this issue.